Probing Anomalous Couplings in Single Higgs Production at ep Collider

Pramod Sharma and Ambresh Shivaji, JHEP 10 (2022) 108

Pramod Sharma

IISER Mohali, India

Electrons for the LHC
Workshop on the LHeC/FCC-eh and PERLE at IJCLab Orsay
Oct 26-28, 2022

- A particle of 125 GeV discovered by CMS and ATLAS experiments in 2012
- So far measurements of Higgs boson properties are compatible with SM within current uncertainties
- The **KEY** to probe new physics is to verify EWSB (Higgs mechanism)
- Uncertainty $\rightarrow \approx 10\,\%$ in Higgs to gauge boson couplings

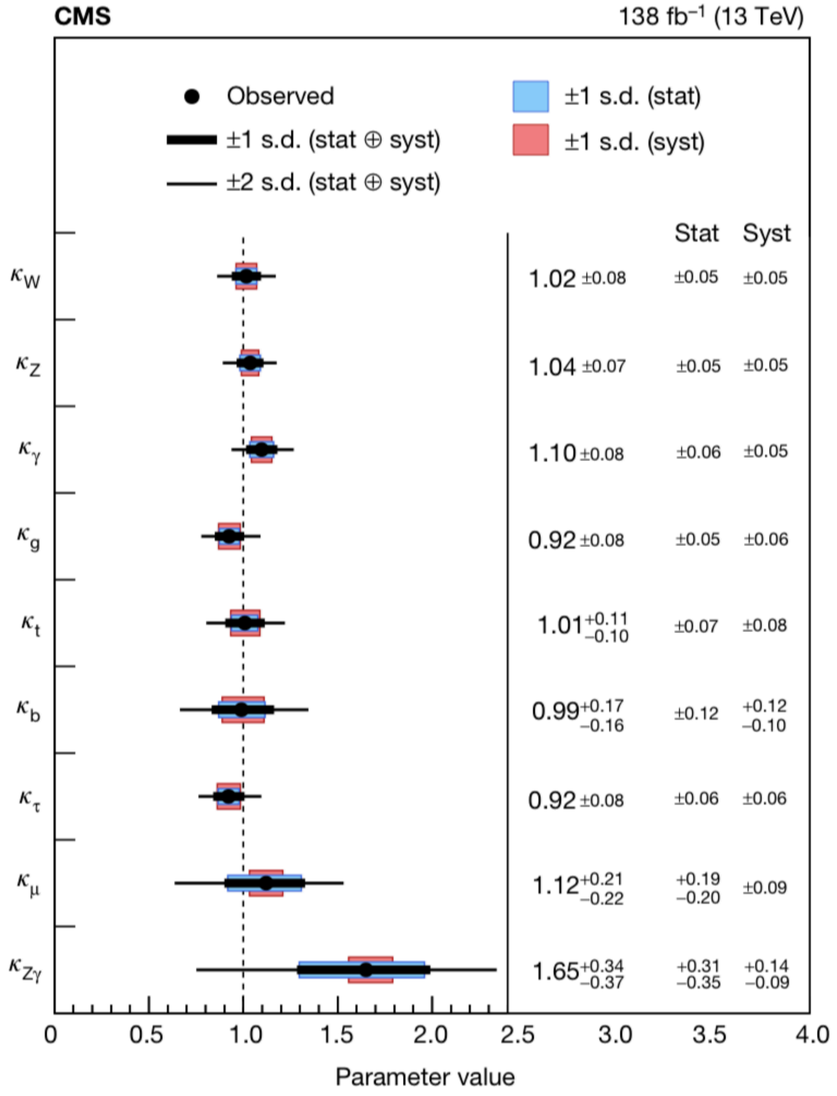

Ref. [1] Nature 607, 60-68 (2022)

Anomalous $HVV(V = W^{\pm}, Z)$ coupling

Most general Lagrangian

$$g\left(m_W \kappa_W W_\mu^+ W^{-\mu} + \frac{\kappa_Z}{2\,\cos\theta_W} m_Z Z_\mu Z^\mu\right) H$$

$$-\frac{g}{m_W}\left[\frac{\lambda_{1W}}{2} W^{+\mu\nu} W^-_{\mu\nu} + \frac{\lambda_{1Z}}{4} Z^{\mu\nu} Z_{\mu\nu}\right.$$

$$+\lambda_{2W}(W^{+\nu}\partial^\mu W^-_{\mu\nu} + h\,.\,c.) + \lambda_{2Z} Z^\nu \partial^\mu Z_{\mu\nu}$$

$$\left.+\frac{\tilde{\lambda}_W}{2} W^{+\mu\nu}\widetilde{W}^-_{\mu\nu} + \frac{\tilde{\lambda}_Z}{4} Z^{\mu\nu}\widetilde{Z}_{\mu\nu}\right] H$$

$g \to SU(2)$ coupling parameter

$$\tilde{V}^{\mu\nu} = \frac{1}{2}\epsilon^{\mu\nu\alpha\beta} V_{\alpha\beta}$$

$$V^{\mu\nu} = \partial^\mu V^\nu - \partial^\nu V^\mu$$

Anomalous $HVV(V = W^{\pm}, Z)$ coupling

Most general Lagrangian

$$g\left(m_W \kappa_W W_\mu^+ W^{-\mu} + \frac{\kappa_Z}{2\cos\theta_W} m_Z Z_\mu Z^\mu\right) H$$

} SM like

$$-\frac{g}{m_W}\left[\frac{\lambda_{1W}}{2} W^{+\mu\nu} W^-_{\mu\nu} + \frac{\lambda_{1Z}}{4} Z^{\mu\nu} Z_{\mu\nu}\right.$$

$$+\lambda_{2W}(W^{+\nu}\partial^\mu W^-_{\mu\nu} + h.c.) + \lambda_{2Z} Z^\nu \partial^\mu Z_{\mu\nu}$$

$$\left.+\frac{\tilde{\lambda}_W}{2} W^{+\mu\nu}\widetilde{W}^-_{\mu\nu} + \frac{\tilde{\lambda}_Z}{4} Z^{\mu\nu}\tilde{Z}_{\mu\nu}\right] H$$

} Derivative of fields

Anomalous $HVV(V = W^{\pm}, Z)$ coupling

Most general Lagrangian

$$g\left(m_W \kappa_W W_\mu^+ W^{-\mu} + \frac{\kappa_Z}{2\cos\theta_W} m_Z Z_\mu Z^\mu\right) H$$

SM like

$$-\frac{g}{m_W}\left[\frac{\lambda_{1W}}{2} W^{+\mu\nu} W^-_{\mu\nu} + \frac{\lambda_{1Z}}{4} Z^{\mu\nu} Z_{\mu\nu}\right.$$

CP even

$$+\lambda_{2W}(W^{+\nu}\partial^\mu W^-_{\mu\nu} + h.c.) + \lambda_{2Z} Z^\nu \partial^\mu Z_{\mu\nu}$$

Derivative of fields

$$\left.+\frac{\tilde{\lambda}_W}{2} W^{+\mu\nu}\widetilde{W}^-_{\mu\nu} + \frac{\tilde{\lambda}_Z}{4} Z^{\mu\nu}\widetilde{Z}_{\mu\nu}\right] H$$

CP odd

Anomalous $HVV(V = W^{\pm}, Z)$ coupling

Most general Lagrangian

$$g\left(m_W \kappa_W W_\mu^+ W^{-\mu} + \frac{\kappa_Z}{2\,\cos\theta_W} m_Z Z_\mu Z^\mu\right) H$$

$$-\frac{g}{m_W}\left[\frac{\lambda_{1W}}{2} W^{+\mu\nu} W^-_{\mu\nu} + \frac{\lambda_{1Z}}{4} Z^{\mu\nu} Z_{\mu\nu}\right.$$

$$+\lambda_{2W}(W^{+\nu}\partial^\mu W^-_{\mu\nu} + h.c.) + \lambda_{2Z} Z^\nu \partial^\mu Z_{\mu\nu}$$

$$\left.+\frac{\tilde{\lambda}_W}{2} W^{+\mu\nu}\widetilde{W}^-_{\mu\nu} + \frac{\tilde{\lambda}_Z}{4} Z^{\mu\nu}\widetilde{Z}_{\mu\nu}\right] H$$

Vertex form

$$\Gamma^{\mu\nu}_{HVV}(p_1, p_2)$$

$$g_V m_V \kappa_V g^{\mu\nu}$$

$$+\frac{g}{m_W}\left[\lambda_{1V}(p_1^\nu p_2^\mu - g^{\mu\nu} p_1 \cdot p_2)\right.$$

$$+\ \lambda_{2V}\,(p_1^\mu p_1^\nu + p_2^\mu p_2^\nu - g^{\mu\nu} p_1 \cdot p_1 - g^{\mu\nu} p_2 \cdot p_2)$$

$$\left.+\ \tilde{\lambda}_V\ \epsilon^{\mu\nu\alpha\beta} p_{1\alpha} p_{2\beta}\right]$$

ep Collider

Collider	COM of mass energy (TeV)	Process	Cross section (pb)
pp	**14**	$pp \to hjj$	**3.7**
ILC	**1**	$e^+e^- \to e^+e^-h$ $e^+e^- \to \nu_e\bar{\nu}_e h$	0.007 0.21
CLIC	**3**	$e^+e^- \to e^+e^-h$ $e^+e^- \to \nu_e\bar{\nu}_e h$	6×10^{-4} 0.5
LHeC	**1.3**	$e^-p \to e^-hj$ $e^-p \to \nu_e hj$	0.016 0.088

- **LHeC:** e^- energy 60 to 120 GeV with 120 GeV proton energy
- Sufficiently large cross section as compared to e^+e^- collider
- Clean environment as with suppressed background as compared to pp collider

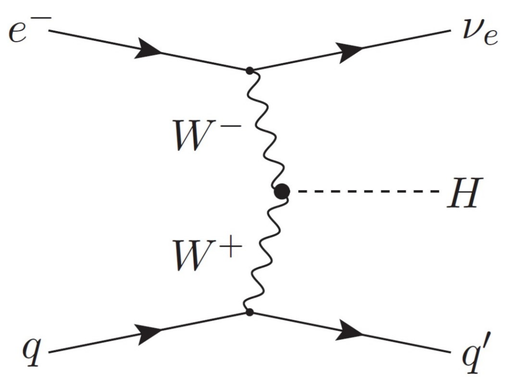

CC

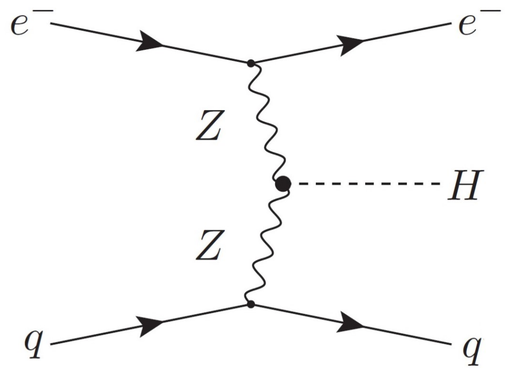

NC

Results and discussion

Observables: $|\Delta\phi|$ is azimuthal correlation of two particles 1 and 2

$$|\Delta\phi| = cos^{-1}(\hat{p}_{T1} \cdot \hat{p}_{T2})$$

Motivation: $|\Delta\phi|$ distribution is a good observable to distinguish CP-even and CP-odd couplings of CC process considered in ref. [2]

Ref. [2]: Phys. Rev. Lett. 109 (2012) 261801, [1203.6285]

Results

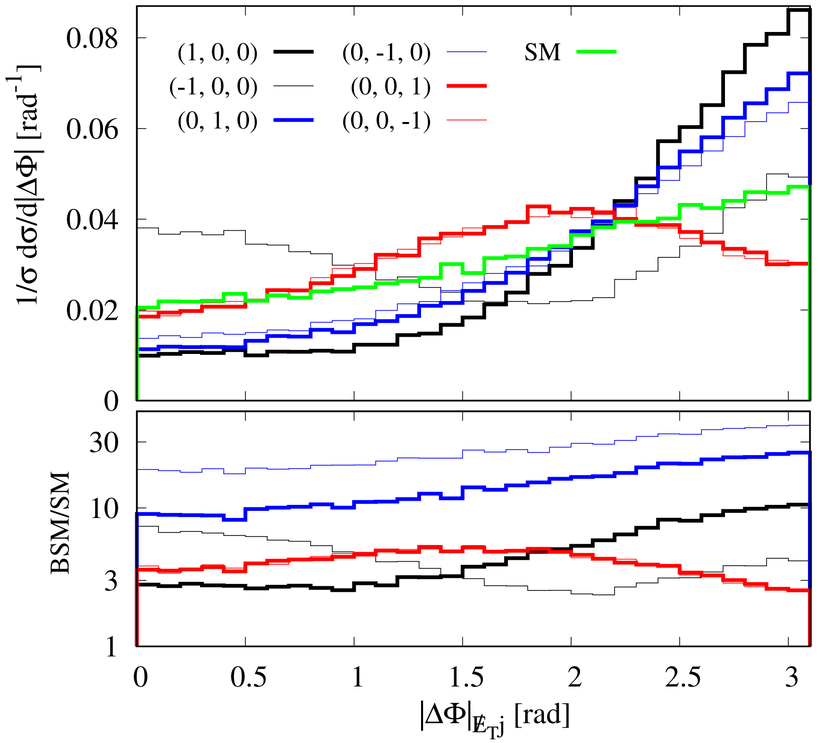

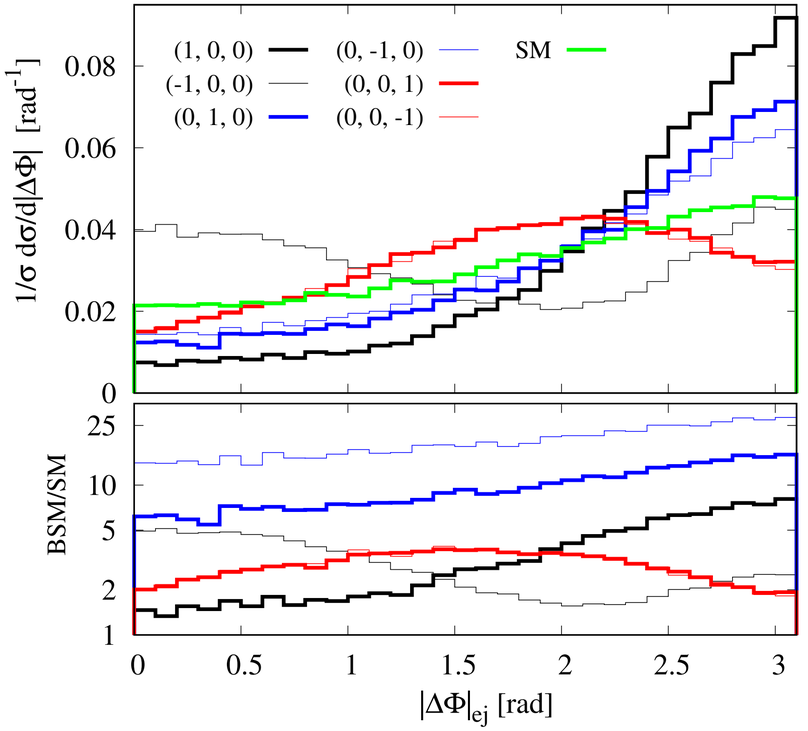

BSM effects in $|\Delta\phi|$ distribution for CC (left) and NC (right)

$(\lambda_{1V}, \lambda_{2V}, \tilde{\lambda}_V)$

- $|\Delta\phi|$ is sensitive to individual effect of new couplings
- Deviation in distribution with respect to SM is largest for λ_{2V} and smallest for $\tilde{\lambda}_V$

Results

Signal for CC (NC) $e^- p \to \nu_e(e^-)hj, h \to b\bar{b}$ $j = g, u, d, s, c$

Results

Signal for CC (NC) $e^- p \to \nu_e(e^-) h j, h \to b\bar{b}$ $j = g, u, d, s, c$

Background for CC (NC)

- Irreducible background : $e^- p \to \nu_e(e^-) b\bar{b} j$

Results

Signal for CC (NC) $e^-p \to \nu_e(e^-)hj, h \to b\bar{b}$ $j = g, u, d, s, c$

Background for CC (NC)

- Irreducible background : $e^-p \to \nu_e(e^-)b\bar{b}j$
- Reducible background:
  - $e^-p \to \nu_e(e^-)jjj$
  - $e^-p \to \nu_e(e^-)bbjj$
  - Photo production from $e^-p \to e^-b\bar{b}j$

$\gamma^*p \to b\bar{b}j$ for CC process

Results

Signal for CC (NC) $e^- p \to \nu_e(e^-) h j, h \to b\bar{b}$ $j = g, u, d, s, c$

Background for CC (NC)

- Irreducible background : $e^- p \to \nu_e(e^-) b\bar{b} j$
- Reducible background:
  - $e^- p \to \nu_e(e^-) jjj$
  - $e^- p \to \nu_e(e^-) bbjj$
  - Photo production from $e^- p \to e^- b\bar{b} j$

Negligible for miss-tagging rates

c jet $\to 0.1$

light jet $\to$0.01

Reduced by $\not{E}_T$ for a very collinear e^- along the beam pipe

$\gamma^* p \to b\bar{b} j$ for CC process

Results

Signal for CC (NC) $e^-p \to \nu_e(e^-)hj, h \to b\bar{b}$ $j = g, u, d, s, c$

Background for CC (NC)

- Irreducible background : $e^-p \to \nu_e(e^-)b\bar{b}j$ ✓
- Reducible background:
  - $e^-p \to \nu_e(e^-)jjj$ — Negligible for miss-tagging rates: c jet $\to 0.1$, light jet $\to 0.01$
  - $e^-p \to \nu_e(e^-)bbjj$ ✓
  - Photo production from $e^-p \to e^-b\bar{b}j$ → $\gamma^*p \to b\bar{b}j$ for CC process

Reduced by $\not{E}_T$ for a very collinear e^- along the beam pipe

Results

Signal for CC (NC) $e^-p \to \nu_e(e^-)hj, h \to b\bar{b}$ $j = g, u, d, s, c$

Background for CC (NC)

- Irreducible background : $e^-p \to \nu_e(e^-)b\bar{b}j$ ✓

Negligible for miss-tagging rates

c jet $\to 0.1$

light jet $\to 0.01$

- Reducible background: $e^-p \to \nu_e(e^-)jjj$

  $e^-p \to \nu_e(e^-)bbjj$ ✓

Energy smearing of partons by $\frac{\sigma_E}{E} = a/\sqrt{E} \oplus b$

a = 0.6, b= 0.04 for jets, a= 0.12, b=0.02 for electrons [3]

Ref [3]: LHeC, FCC-he Study Group collaboration, J. Phys. G 48 (2021) 110501,[2007.14491].

Results

Signal v/s background

Cuts or **CC**

$$p_T(j) > 30\ GeV,\ p_T(b) > 30\ GeV,\ \not{E}_T > 25 GeV$$

$$|M_{b\bar{b}} - m_H| < 15\ GeV$$

$$1 < \eta_j < 5.0,\ -1 < \eta_b < 4.0,\ M_{Hj} > 250\ GeV$$

Process	Events at generation level	Events after cuts
Signal	3011	819
$\nu_e b\bar{b}j$	18883	30
$\nu_e b\bar{b}jj$	10985	38
S/B	0.1	12.0

Cuts or **NC**

$$p_T(e) > 20\ GeV,\ p_T(j) > 30\ GeV,\ p_T(b) > 30\ GeV$$

$$|M_{b\bar{b}} - m_H| < 15\ GeV$$

$$|\eta_e| < 2.5,\ 2 < \eta_j < 5.0,\ 0.5 < \eta_b < 4.0,\ M_{Hj} > 300\ GeV$$

Process	Events at generation level	Events after cuts
Signal	534	76
$e^- b\bar{b}j$	2.75×10^6	161
$e^- b\bar{b}jj$	6.3×10^5	24
S/B	0.02×10^{-2}	0.41

Results

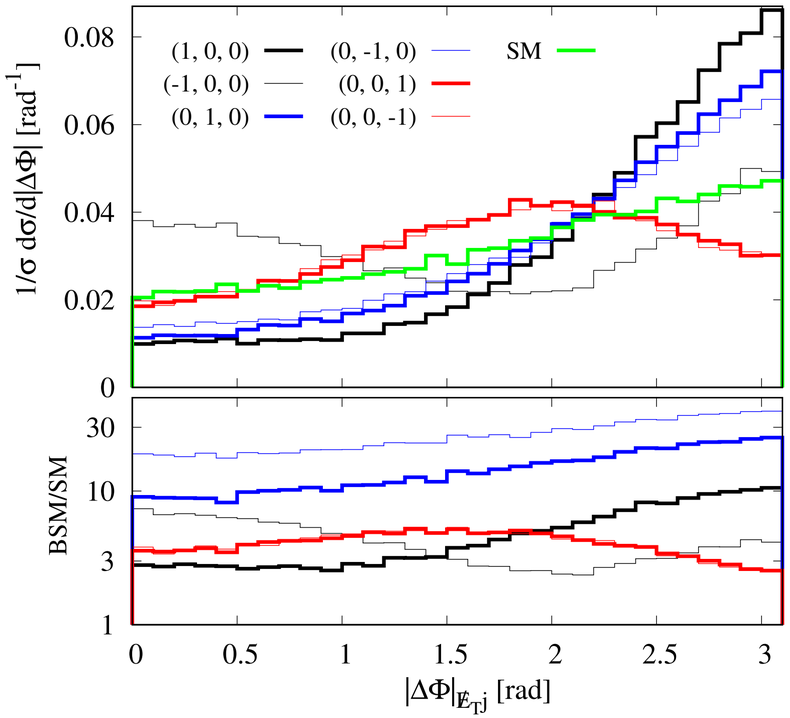

Constraints on HWW parameters at $L = 100\ fb^{-1}$

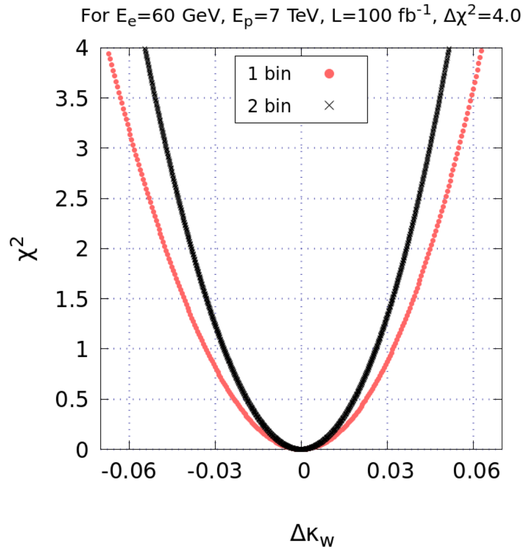

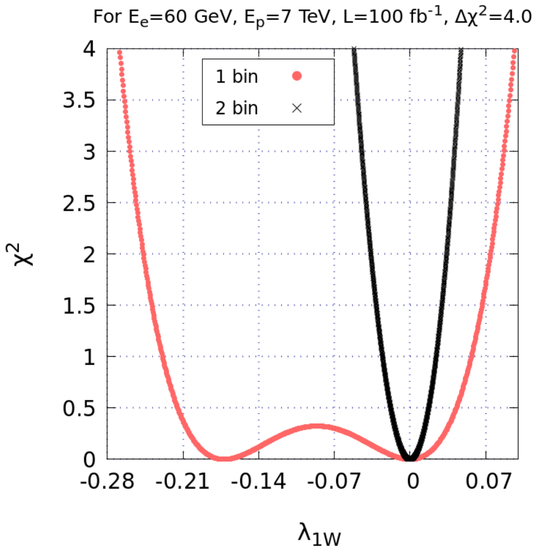

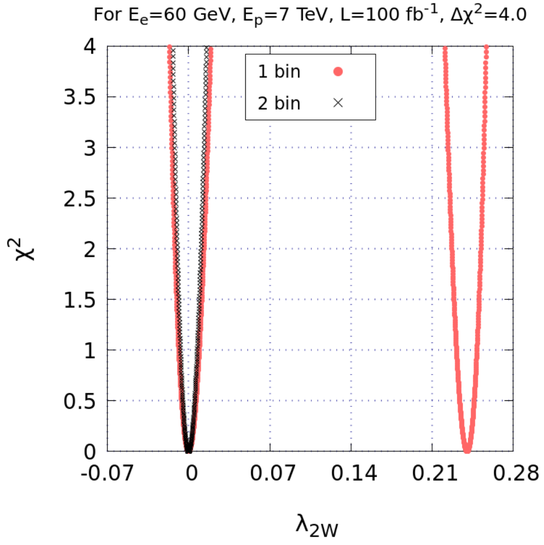

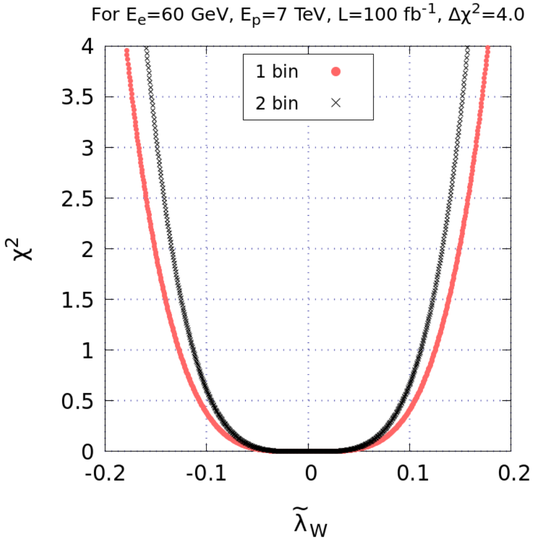

- λ_{2W} is considered most while $\tilde{\lambda}_W$ is constrained least
  - Very small effect of 2 bin analysis on κ_W and $\tilde{\lambda}_W$

at 95% C.L.

	Our limits at $L = 100\ fb^{-1}$			
$\kappa_W \rightarrow$	[0.94,1.05]	Run II data [a] $35.9\ fb^{-1}$, 13 TeV [0.76,1.34]	HL LHC [e] 3.4%	CLIC [f] $1\ ab^{-1}$, 350 GeV 1.6%
$\widetilde{\lambda}_W \rightarrow$	[-0.16, 0.16]	Run II LHC [b] $[-0.42,0.3]$	FCC eh [d] $1\ ab^{-1}$, 3.5 TeV [-1.2, 1.2]	LHeC [c] $0.5\ ab^{-1}, E_e = 140$ GeV, $E_p = 6.5$ GeV [-0.2, 0.3]
$\lambda_{1W} \rightarrow$	[-0.05, 0.05]		FCC eh [d] [-0.56, 0.54]	LHeC [c] [-0.06, 0.1]
$\lambda_{2W} \rightarrow$	[-0.013, 0.015]	FCC eh [d] [-0.05, 0.05]		

[a] Eur. Phys. J. C 79 (2019) 421 [arXiv:1809.10733]

[b] Phys. Lett. B 805 (2020) 135426 [arXiv:2002.05315]

[c] arXiv:1203.6285

[d] arXiv:1509.04016

[e] arXiv:1902:00134

[f] arXiv:1812:01644

Constraints on HWW parameters at $L = 100\ fb^{-1}$

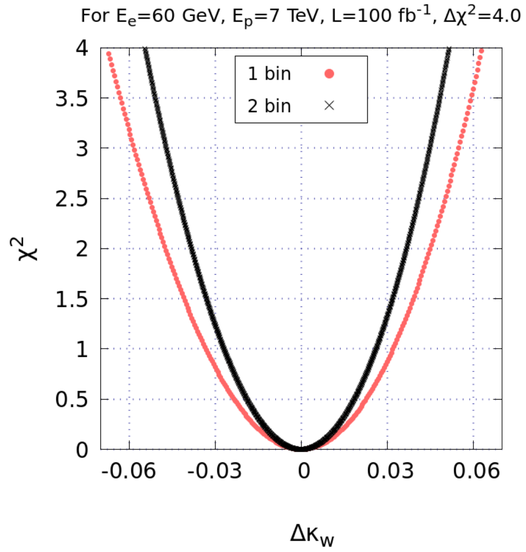

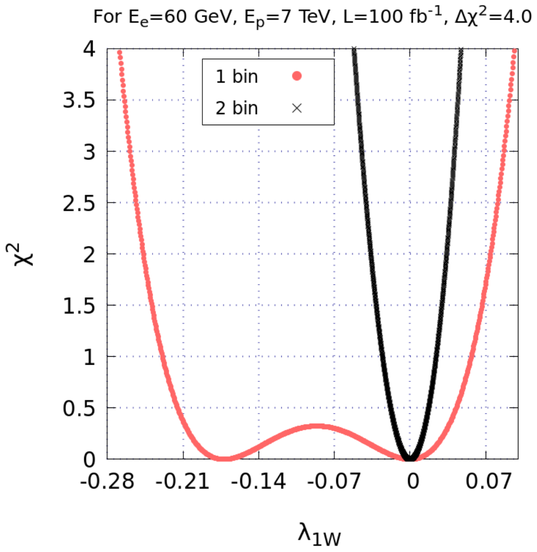

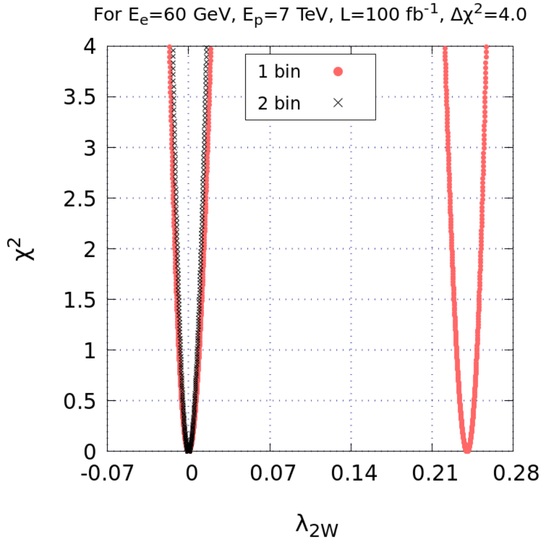

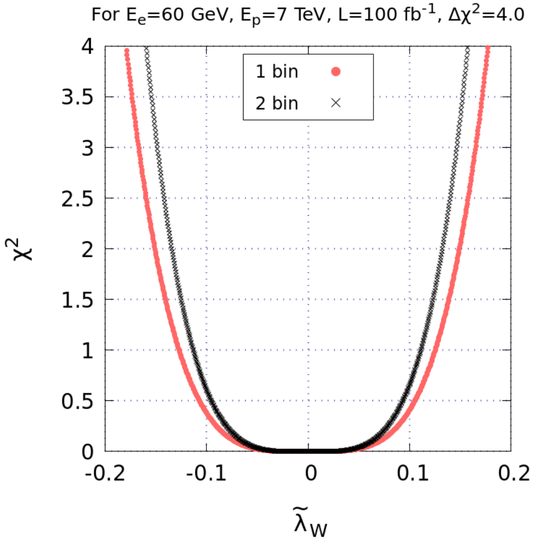

Results

$$\chi^2(c_i) = \sum_{j=1}^{n} \left(\frac{N_j^{\mathrm{BSM}}(c_i) - N_j^{\mathrm{SM}}}{\Delta N_j} \right)^2$$

Suppress χ^2 due to huge background

Constraints on HZZ parameters at $L = 100\ fb^{-1}$

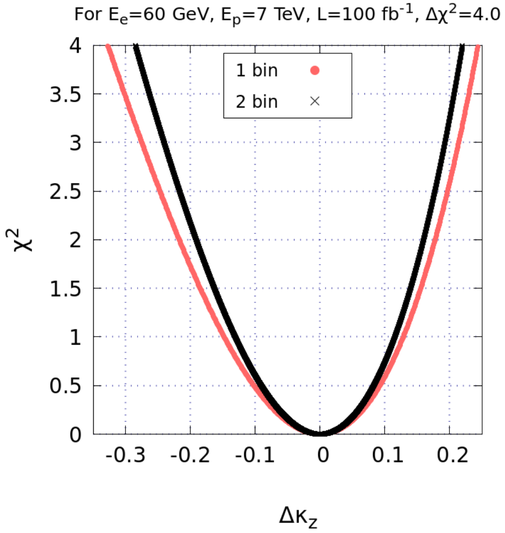

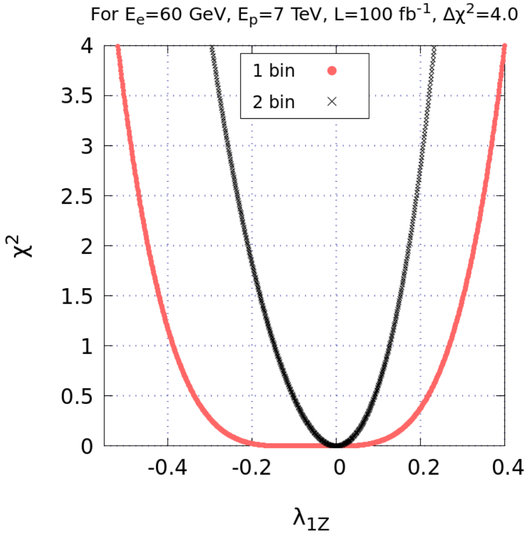

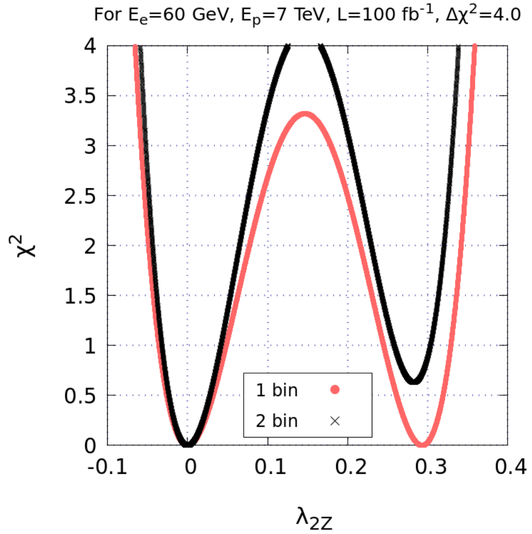

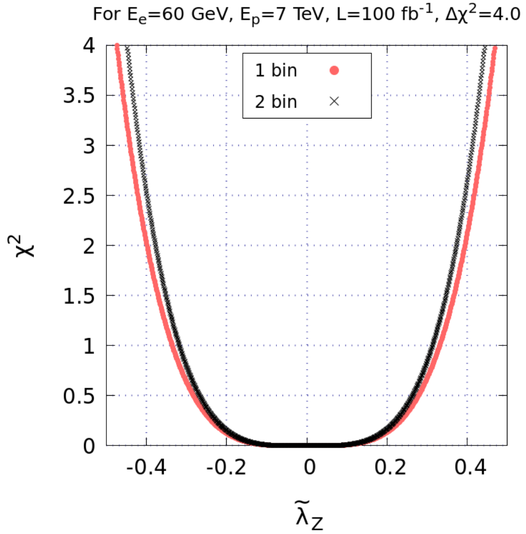

- HZZ parameters less stringent as compared to HWW parameters
- All parameters lie within range [-0.45, 0.45]

at 95% C.L.

	Our limits at $L = 100\ fb^{-1}$			
$\kappa_Z \rightarrow$	[0.72 1.22]	Run II data [a] [0.75, 1.21]	HL LHC [e] 3.0%	CLIC [f] $1\ ab^{-1}$, 350 GeV 0.8%
$\lambda_{1Z} \rightarrow$	[-0.35, 0.25]		HL LHC [g] [-0.01, 0.01]	
$\lambda_{2Z} \rightarrow$	[-0.06,0.13] ∪ [0.17, 0.34]		HL LHC [g] [-0.007, 0.007]	
$\widetilde{\lambda}_Z \rightarrow$	[-0.45, 0.45]	Run II LHC [b] $[-0.21, 0.15]$	HL LHC [g] [-0.08, 0.08]	

[g] JHEP 01 (2018) 096 [arXiv:1703.06667]

Constraints on HWW parameters at $L = 100\ fb^{-1}$

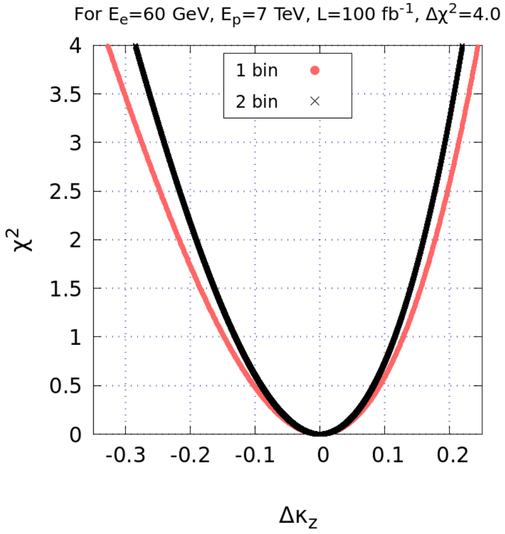

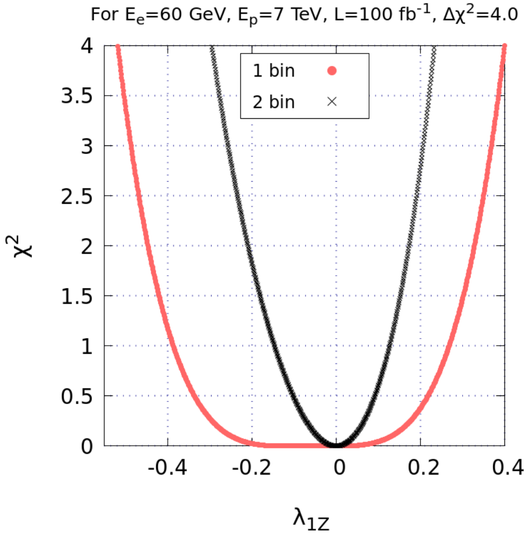

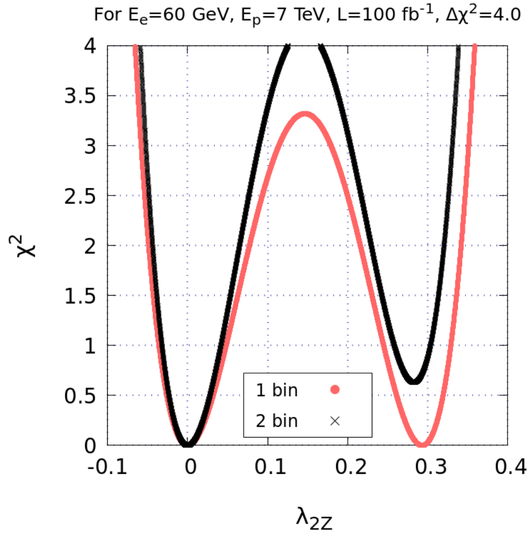

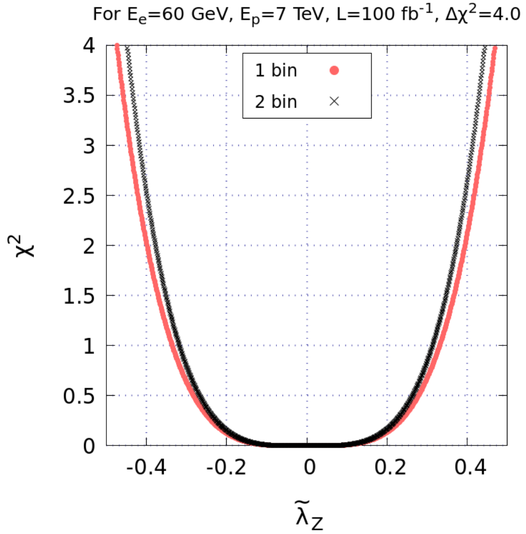

Results

$$\Delta N \approx \sqrt{\sigma L} \quad (\text{for } \delta_{sys} = 0) \implies \chi^2 \propto L$$

at 95% C.L.

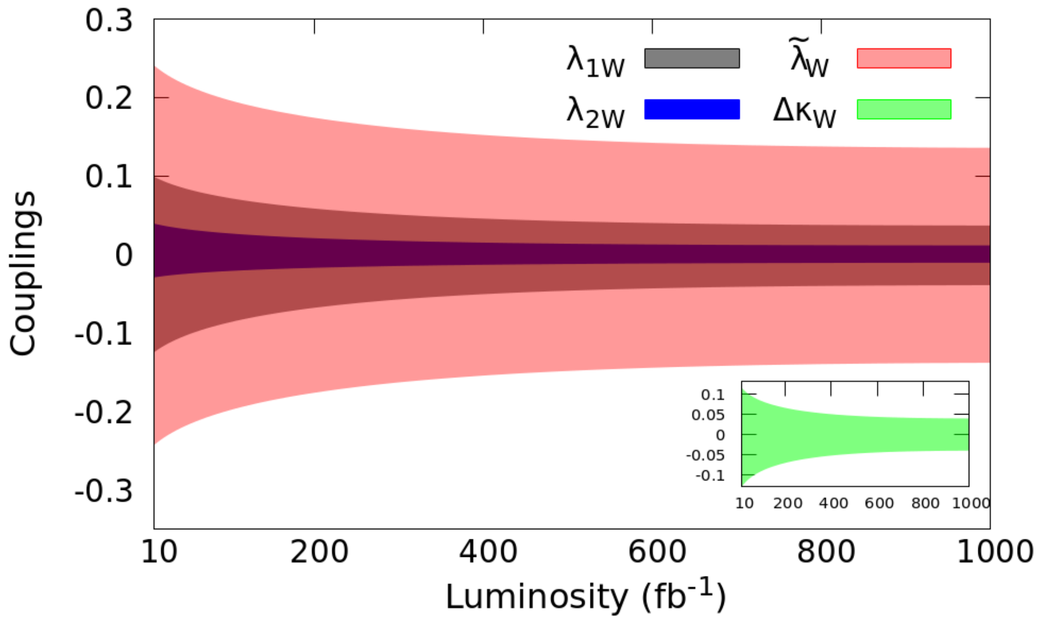

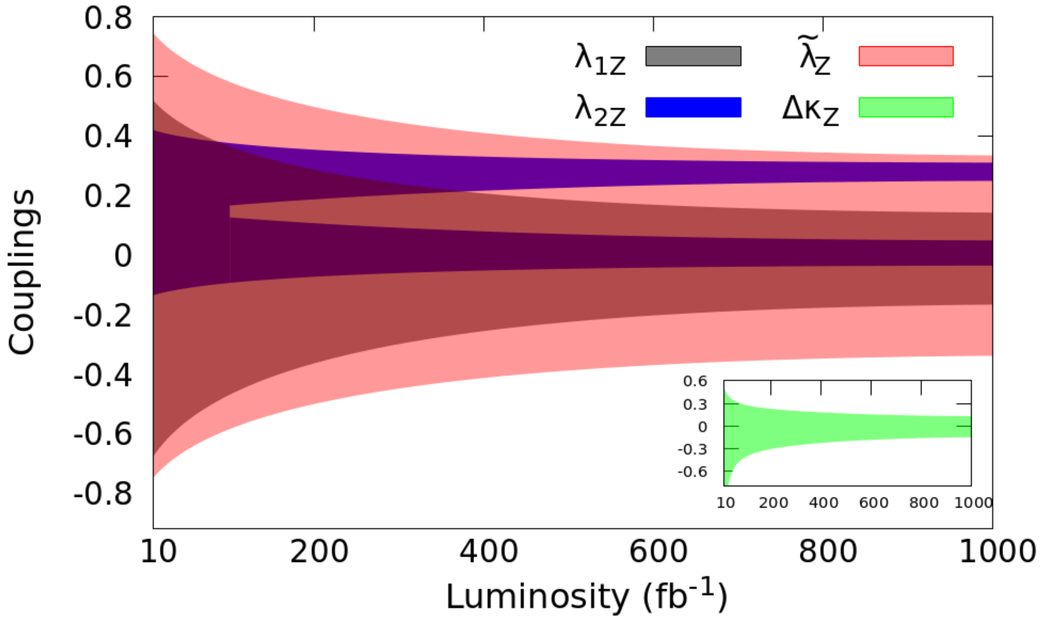

Luminosity from 10 to $10^3\ fb^{-1}$

$$\kappa_W,\ \lambda_{1W},\ \lambda_{2W},\ \tilde{\lambda}_W \rightarrow 67\,\%\,,40\,\%\,,78\,\%\,,42\,\%$$

$$\kappa_Z,\ \lambda_{1Z},\ \lambda_{2Z},\ \tilde{\lambda}_Z \rightarrow 91\,\%\,,74\,\%\,,73\,\%\,,55\,\%$$

Results

two parameter analysis for HWW coupling

$$X^{\mathrm{BSM}} = X^{\mathrm{SM}} + \sum_i X_i c_i + \sum_{i,j} X_{ij} c_i c_j \,.$$

Correlation of two BSM parameters

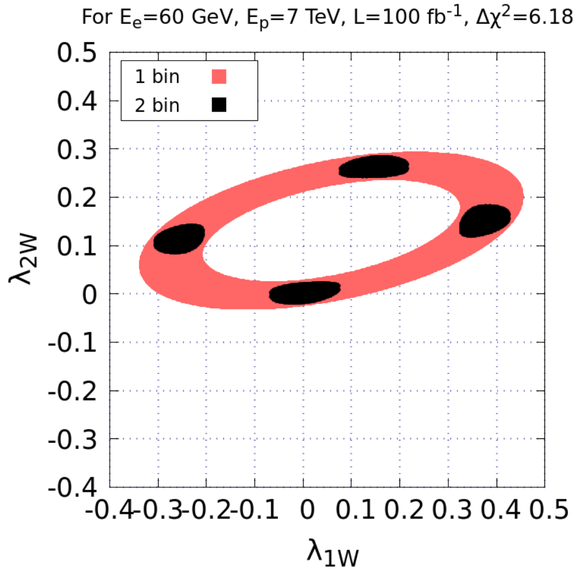

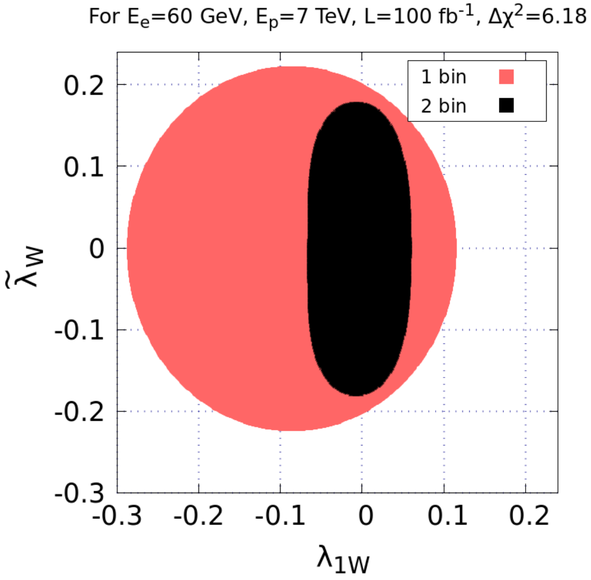

- Parameter space increases as going from one parameter to two parameter analysis
- $(\lambda_{1W}, \lambda_{2W})$ region is strongly correlated
- $(\lambda_{2W}, \tilde{\lambda}_W)$ region has least effect of 2 bin analysis

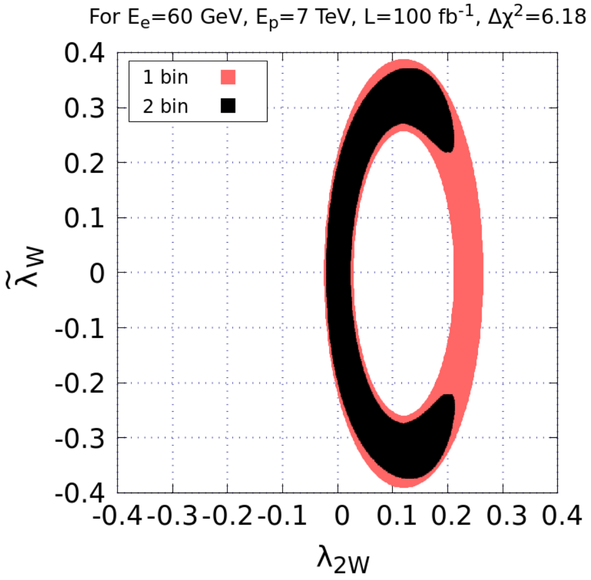

Results

two parameter analysis for HWW coupling

$$X^{\mathrm{BSM}} = X^{\mathrm{SM}} + \sum_i X_i c_i + \sum_{i,j} X_{ij} c_i c_j \,.$$

Correlation of two BSM parameters

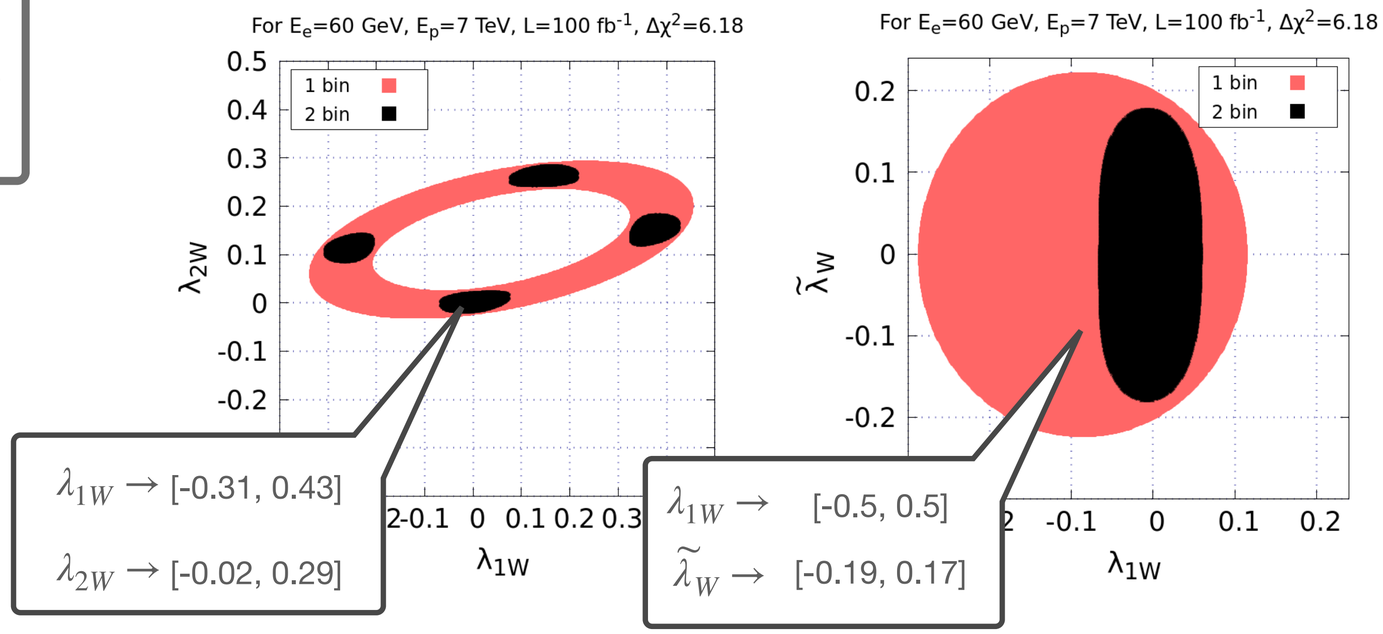

- Parameter space increases as going from one parameter to two parameter analysis
- $(\lambda_{1W}, \lambda_{2W})$ region is strongly correlated
- $(\lambda_{2W}, \tilde{\lambda}_W)$ region has least effect of 2 bin analysis

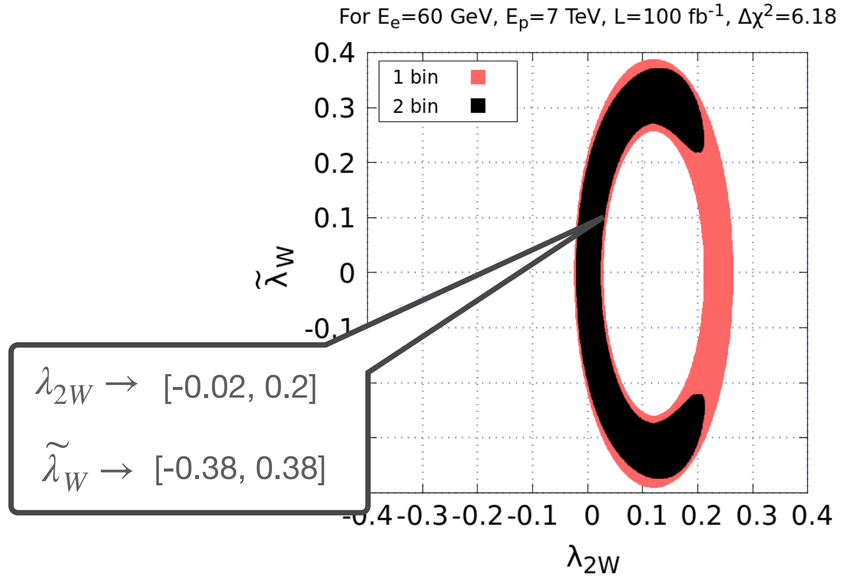

Results

two parameter analysis for HZZ coupling

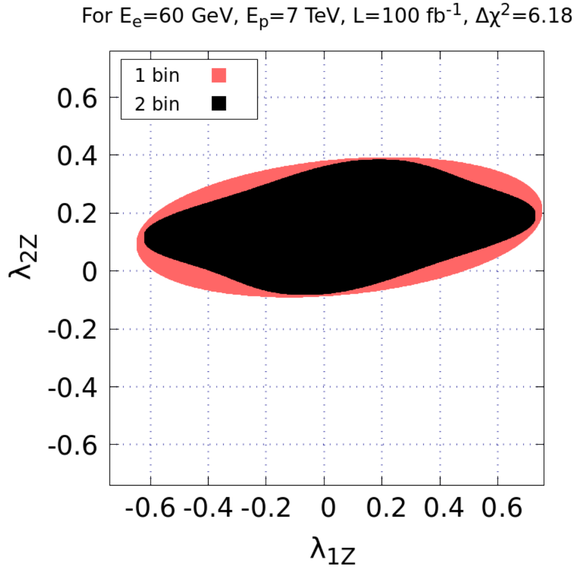

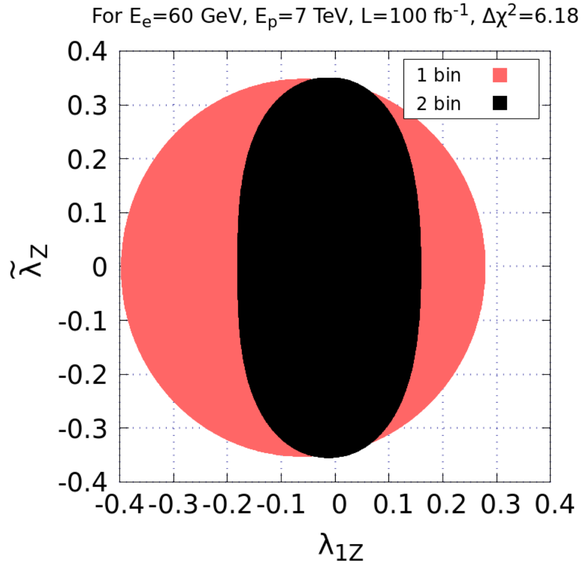

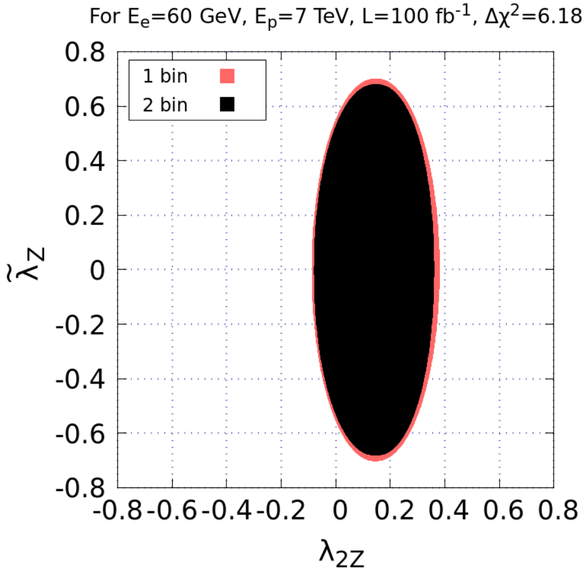

- 2 bin analysis is not efficient to improve constraints
- Like HWW case, $(\lambda_{1Z}, \lambda_{2Z})$ region is also strongly correlated
- $(\lambda_{2Z}, \tilde{\lambda}_Z)$ region has least effect of 2 bin analysis

Results

two parameter analysis for HZZ coupling

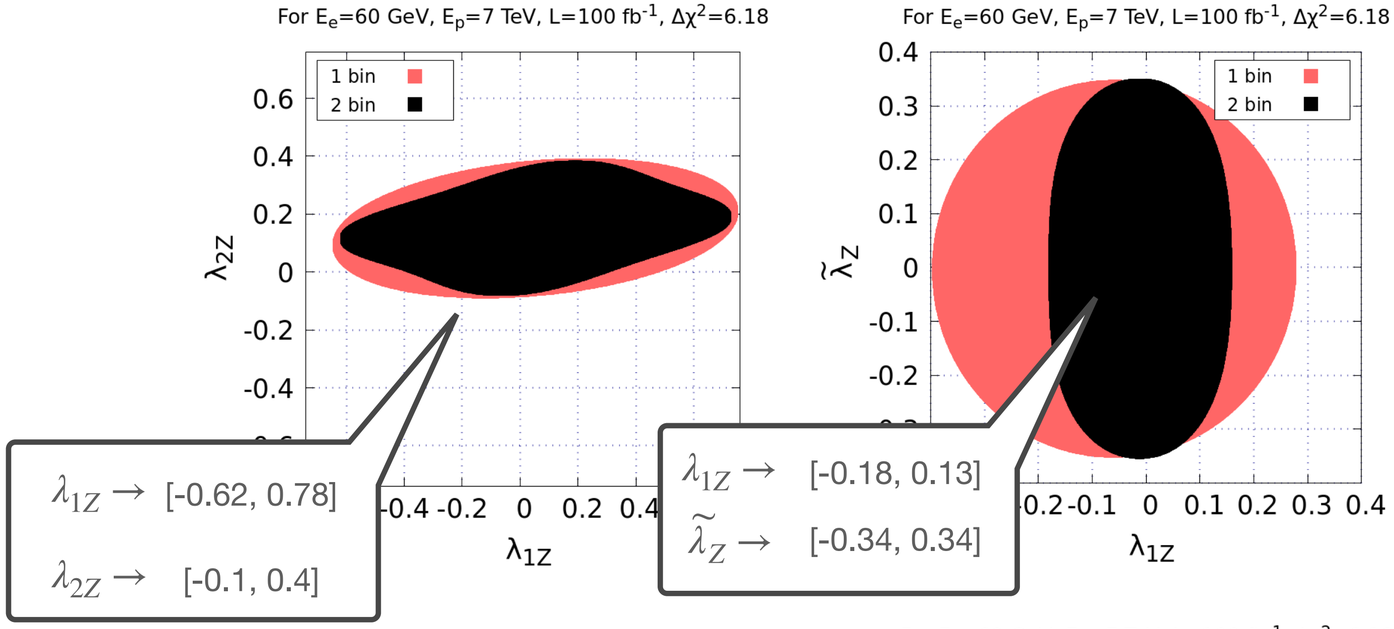

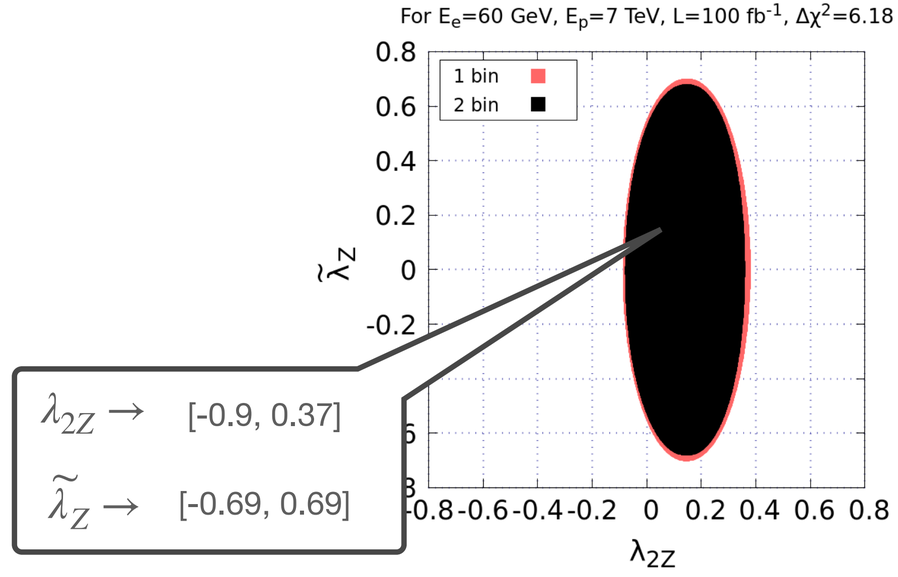

- 2 bin analysis is not efficient to improve constraints
- Like HWW case, $(\lambda_{1Z}, \lambda_{2Z})$ region is also strongly correlated
- $(\lambda_{2Z}, \tilde{\lambda}_Z)$ region has least effect of 2 bin analysis

Conclusion

- $|\Delta\phi|$ distribution is sensitive to $HVV(V = W^{\pm}, Z)$ coupling.
- Using $|\Delta\phi|$ distribution, constraints are obtained keeping one parameter and two parameters non zero at a time.
- Constraints on BSM parameters are improved as going from 1 bin to 2 bin.
- Change in constraints as a function of luminosity is discussed.
- Constraints from two parameter analysis are loose as compared to one parameter analysis.

Back up

For BSM parameter c_i, χ^2 function is

$$\chi^2(c_i) = \sum_{j=1}^{n} \left(\frac{N_j^{\mathrm{BSM}}(c_i) - N_j^{\mathrm{SM}}}{\Delta N_j} \right)^2$$

N_j^{SM} and $N_j^{BSM} \rightarrow$ SM and BSM events in j^{th} bin

uncertainty (Statistical + systematic)

$$\Delta N_j = \sqrt{N_j^{\mathrm{SM+Bkg}} \left(1 + \delta_{sys}^2 N_j^{\mathrm{SM+Bkg}} \right)}$$

5%

$$\sqrt{N_j^{SM+Bkg}} = \sqrt{\sigma_j^{SM+Bkg}\, L}$$

Back up

- $e^- p \to \nu_e b \bar{b} jj$ has 2 events after cuts

- $e^- p \to e^- jjj$ has 15 events and S/B changes 0.41 to 0.38

- PDF: NN23LO1

Uncertainty: 2.5%

- Renormalisation factorisation scale choice: -1 in MadGraph which is related to the transverse energy of the final state particles

Uncertainty: 5%

Back up

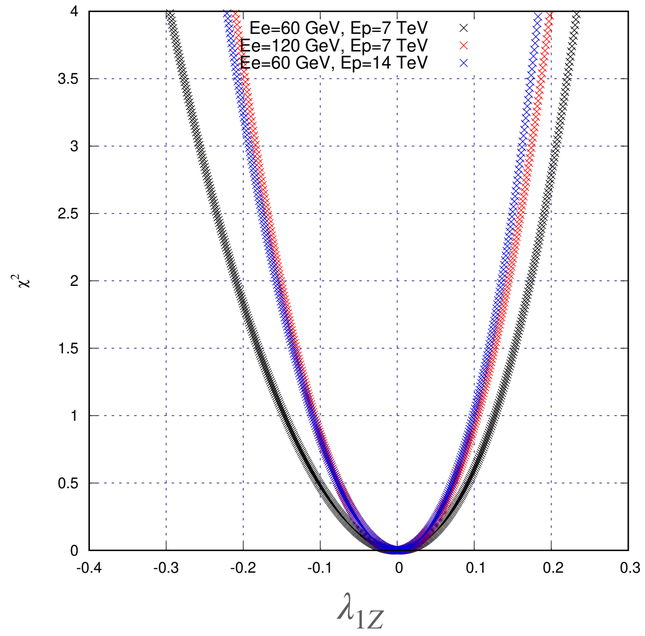

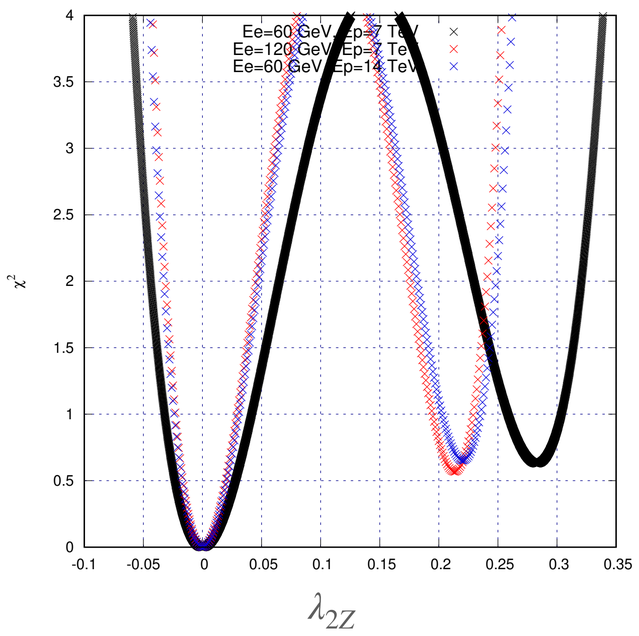

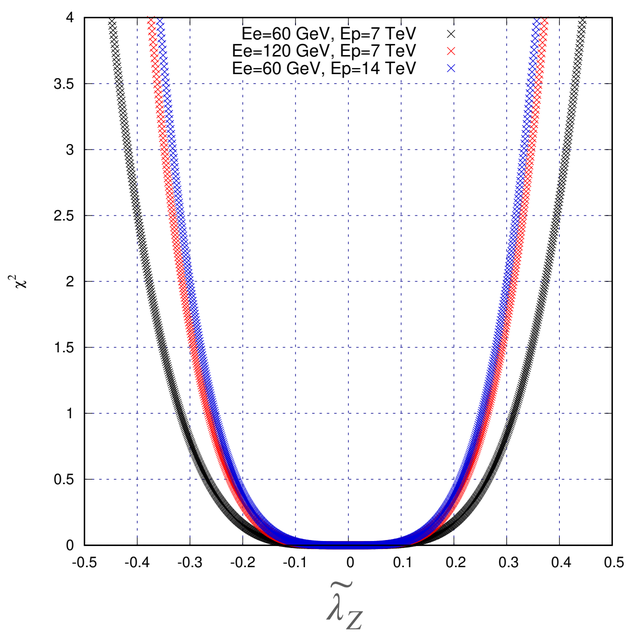

Constraints on HZZ parameters with respect to energy

- Constraints are improved by increasing energy

Back up

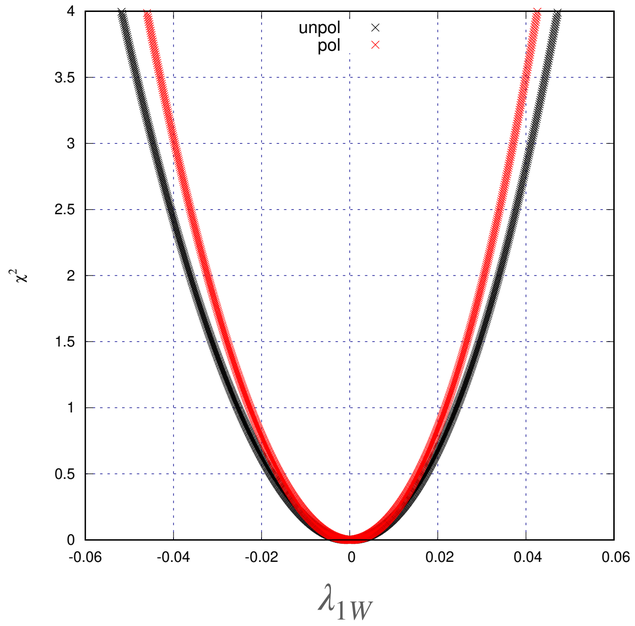

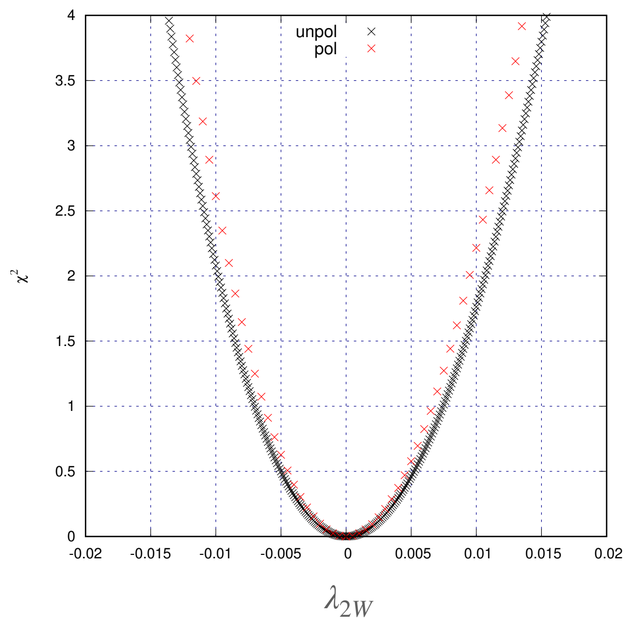

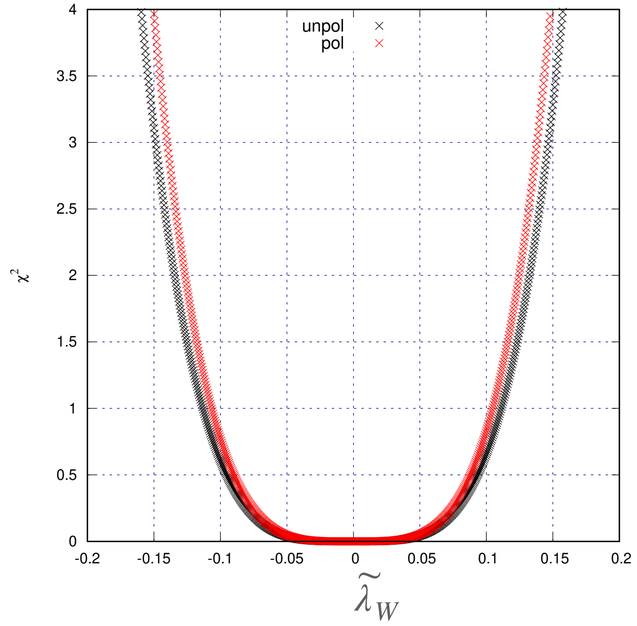

Constraints on HWW parameters for -80% e-beam polarisation

- For -80% e-beam polarization S/B =11.0 (CC) and 0.3 (NC)

No significant improvement in NC but constraints improved by 7-10% in CC case.